Reprinted from JOURNAL OF THE AERONAUTICAL SCIENCES

MARCH, 1956 VOLUME 23, No. 3

The Divergence of Supersonic Wings Including Chordwise Bending*

M. A. BIOT†
Cornell Aeronautical Laboratory, Inc.

ABSTRACT

The static aeroelastic stability or divergence problem is investigated for thin supersonic wings when not only the spanwise bending and twist are taken into account but also the chordwise bending. The problem is treated in successive phases of increasing complexity from the two-dimensional curling-up of the leading edge to the three-dimensional stability of the cantilever wing. Several methods of approach are developed including the nonlinear aspects of the structure and the aerodynamics. Results indicate a strong dependence of stability on Poisson's ratio and the magnitude of the deformation.

INTRODUCTION

THE PROBLEM OF STATIC AEROELASTIC stability or divergence is usually dealt with by introducing certain simplifying assumptions, including that the wing structure is rigid along the direction of the ribs. The advent of supersonic flight and the use of very thin wings requires a re-examination of the problem and the inclusion of chordwise bending in the analysis. The present paper is a review of the investigation of this problem in the supersonic speed range carried out during the past years by the Cornell Aeronautical Laboratory. Many details of the analysis had to be omitted because of space limitations. For specific treatments of each problem the reader is referred to the C.A.L. reports listed in the references.‡

The methods are developed with the assumptions of a lift proportional to the local slope. However, for cases when this assumption does not constitute a valid approximation, this is not a limitation, since three-dimensional aerodynamic theory may readily be introduced by evaluating the corresponding generalized aerodynamic forces. Linear aerodynamic theory is also used in most cases, but it is shown how modification of certain coefficients makes it possible to account for wing thickness and nonlinear effects of aerodynamic origin. The nonlinear elastic behavior of the wing due to finite deformation and the generation of membrane stresses are also discussed.

The theory is developed by considering a succession of cases of increasing complexity. The "curling-up" of a leading edge facing a supersonic stream is treated in Sections (1) and (3) as a two-dimensional problem. Section (1) deals with the stability of a wedge-shaped profile and Section (3) with that of a biconvex profile. Section (2) deals with the deflection of a wedge under conditions of stability but with an initial angle of attack. This introduces the concept of amplification factor, which is a measure of the increase in lift and overturning moment caused by the elasticity of the structure. The results that are made to include the significant features of the nonlinear aerodynamic theory are used to extend the analysis to the three-dimensional problem as developed in Section (4) by a procedure designated as the "strip method." This method is first developed in a simplified form by neglecting the anticlastic effect produced by Poisson's ratio. However, extension of the strip method in Section (7) to include both the anticlastic and nonlinear effects shows that, although the anticlastic effect has a strong influence on the stability for infinitesimal deformations, this influence tends to vanish rapidly for deflections of the order of the wing thickness. This fact enhances considerably the practical importance of the simplified strip method. In Section (5) the equations are solved rigorously on the basis of the theory of plates of uniform thickness and results compared to that of the approximate theory. Section (6) treats the cantilever wings of double wedge section by a method of generalized coordinates. The success of this latter approach depends, of course, entirely on the suitable choice of the coordinates, a choice that is made possible by proper interpretation of previous results. The results that are valid only for infinitesimal deflections show a strong dependence of the stability on Poisson's ratio. This is a consequence of the influence of Poisson's ratio on the anticlastic curvature of the wing in bending. The nonlinear aspects of the theory are discussed in Section (7), and it is shown that the membrane stresses set up by the finite deflection greatly minimize the anticlastic effect as soon as the magnitude of the deflection becomes of the order of the wing thickness. The theory is developed by extending the simplified strip method of Section (4) to include the anticlastic effect. For small deflections the twist is shown to satisfy an ordinary differential equation of the fourth order along the span, and the nonlinearity appears as a modification of the coefficients in this equation. This approach has also the advantage of lumping all the variables of the prob-

---

Presented at the Aeroelasticity Session, Twenty-Third Annual Meeting, IAS, New York, January 24–27, 1955.

* The writer is indebted to Mr. A. Donovan of the Cornell Aeronautical Laboratory for suggesting this investigation and to Messrs. S. Slutsky and M. Kochen for assistance in the analytical and numerical work. The investigation was carried out partly under the sponsorship of the Bureau of Ordnance, US Navy, as part of Contract NOrd-10057.

† Consultant.

‡ Requests for these reports should be addressed to Cornell Aeronautical Laboratory, Inc., Box 235, Buffalo 21, N. Y.

lem into two basic parameters. The influence of nonlinear aerodynamics is also discussed in this section, and appropriate correction factors are introduced which depend upon the Mach Number and the wing thickness.

The present theory must be considered as a first step yielding information on the nature of significant parameters, an evaluation of the efficiency of various methods of calculation, and simple procedures for the approximate determination of the stability. The results should be particularly useful in choosing appropriate generalized coordinates and procedures for accurate computation with automatic computers.

It should also be noted that the methods and equations derived in the present theory cover a wider field than just the divergence problem since they are directly applicable to the calculation of aeroelastic stability derivatives required in problems of control.

(1) The Leading-Edge Instability

Before we attempt to deal with the stability of the wing as a whole, it is essential to analyze the properties of the leading edge of a supersonic wing from the standpoint of its aeroelastic stability. It will be shown here that it exhibits an instability of its own such that for zero angle of attack it tends to "curl-up."

This phenomenon admits of an exact analysis by considering a cylindrical wedge of trapezoidal section symmetric about its center line, whose thick edge of thickness h is clamped while the thin edge of thickness ah is facing a stream of supersonic velocity V, as shown in Fig. 1.

The chord of the wedge is l. When the wedge is undeformed, there is no lift on the structure. The problem is to examine the stability of this structure with the assumption that it is an elastic, isotropic, and homogeneous solid.

The problem has been given detailed treatment in reference 2. The wedge structure is considered as a beam while the aerodynamic forces are derived from the two-dimensional linear supersonic theory—i.e., the local lift is assumed proportional to the local slope of the center line. The local lift per unit area is

$$q = -(4M^2/\sqrt{M^2 - 1})(\rho c^2/2)\,(dw/dx) \qquad (1.1)$$

where w = the upward deflection of the center line, ρ = air mass density, c = velocity of sound, and $M = V/c$ = Mach Number. The wedge deflection equation is

$$(d^2/dx^2)\,[E_1 I(d^2w/dx^2)] = q \qquad (1.2)$$

with $E_1 = E/(1 - \nu^2)$ a "reduced" Young's modulus for two-dimensional strain, E = Young's modulus, ν = Poisson's ratio, and I = moment of inertia per unit span of the cross section about a spanwise axis through its center line.

The x axis lies along the direction of the stream velocity, V, and it is convenient in the present problem to place the origin at the intersection of the top and bottom faces of the wedge. The moment of inertia may then be written

$$I = h^3x^3/(12l_1^3) \qquad (1.3)$$

with

$$l_1 = l/(1 - a) \qquad (1.4)$$

Combining Eqs. (1.1), (1.2), and (1.3), we may write the stability equation as

$$(d^2/d\xi^2)\,[\xi^3(d\alpha/d\xi)] + k_1\alpha = 0 \qquad (1.5)$$

The nondimensional variables are

$$\xi = x/l_1$$

$$\alpha = -\,dw/dx$$

and the stability parameter is

$$k_1 = 24\,(M^2/\sqrt{M^2 - 1})\,(\rho c^2/E_1)\,(l_1/h)^3 \qquad (1.6)$$

It is readily seen that Eq. (1.5) is not of the self-adjoint type. The present eigenvalue problem, therefore, differs essentially from the usual vibration or elastic stability problem. The general solution for Eq. (1.5) is

$$\alpha = C_1\xi^{m_1} + C_2\xi^{m_2} + C_3\xi^{m_3} \qquad (1.7)$$

where

$$m_i = z_i - 1; \quad i = 1, 2, 3 \qquad (1.8)$$

and z_i are the three roots of the cubic equation

$$z(z^2 - 1) + k_1 = 0 \qquad (1.9)$$

This equation has a real root

$$z_1 < -1$$

The two other roots may be expressed in terms of z_1 as

$$\left.\begin{aligned} z_2 &= -(z_1/2) + (1/2)\sqrt{4 - 3z_1^2} \\ z_3 &= -(z_1/2) - (1/2)\sqrt{4 - 3z_1^2} \end{aligned}\right\} \qquad (1.10)$$

The latter roots are complex conjugates if

$$k_1 > 2/(3\sqrt{3}) = 0.3849 \qquad (1.11)$$

In this case, also $z_1 < -2/\sqrt{3} = -1.1548$.

Introducing the general solution, Eq. (1.7), into the three boundary conditions

$$\left.\begin{aligned} \alpha = 0 \quad &\text{for } \xi = 1 \\ \xi^3(d\alpha/d\xi) = (d/d\xi)\,[\xi^3(d\alpha/d\xi)] = 0 \quad &\text{for } \xi = a \end{aligned}\right\} \qquad (1.12)$$

we find a characteristic equation that may be written in two different forms depending on whether the roots, z_2 and z_3, are real or complex.

In the first case—i.e., for $k_1 < 0.3849$—the characteristic equation is

$$\frac{Bz_1(z_1 + 1)}{z_1 - 1}\left(\frac{1}{a}\right)^{3z_1/2} + \frac{2 + 3z_1}{2}\sinh\left(B\log\frac{1}{a}\right) + B(2z_1 + 1)\cosh\left(B\log\frac{1}{a}\right) = 0$$

with

$$B = (1/2)\sqrt{4 - 3z_1^2} \qquad (1.13)$$

For a given value of a, this may be considered an equation for the characteristic parameter k_1. It is easily verified that for values of a such that

$$0 < a < 1$$

there are no real roots k_1 since all three terms of Eq. (1.13) are always negative. Hence we must have $k_1 > 0.3849$ and the characteristic equation becomes

$$\frac{B'z_1(z_1+1)}{z_1-1}\left(\frac{1}{a}\right)^{3z_1/2} + \frac{2+3z_1}{2}\sin\left(B'\log\frac{1}{a}\right) + B'(2z_1+1)\cos\left(B'\log\frac{1}{a}\right) = 0$$

with

$$B' = (1/2)\sqrt{3z_1^2 - 4} \qquad (1.14)$$

This equation has an infinite number of roots corresponding to different modes of instability. The lowest value of k_1 corresponds to the mode of lowest stability. Eq. (1.14) may be solved for this value of k_1 as a function of a. Actually, we choose to refer the stability parameter to the actual chord l instead of l_1. The corresponding stability parameter is then

$$k = 24\,(M^2/\sqrt{M^2-1})\,(\rho c^2/E_1)\,(l/h)^3 \qquad (1.15)$$

This parameter is related to k_1 by the relation

$$k = k_1(1-a)^3 \qquad (1.16)$$

The lowest critical value, k_c, of k versus a is given by Table 1. This value of k_c versus a is plotted in Fig. 3 as the curve marked A.

The limiting value $k = 6.33$ for $a = 1$ has been calculated directly from the case of a slab of uniform thickness—i.e., by solving the simple equation

$$(d^3\alpha/d\xi^3) + k\alpha = 0 \qquad (1.17)$$

with $\xi = x/l$

It remains to be seen what the stability becomes in the case of $a = 0$. This corresponds to either the case of an infinite chord or an infinitely sharp leading edge. It is seen that the boundary conditions are

$$\alpha = 0 \quad \text{for } \xi = 1$$

$$\xi^3(d\alpha/d\xi) = (d/d\xi)\,[\xi^3(d\alpha/d\xi)] = 0 \quad \text{for } \xi = 0 \qquad (1.18)$$

The last two conditions are satisfied if any of the exponents, m_i, appearing in the general solution, Eq. (1.7), is such that

$$\text{Re}\,(m_i) > -1^* \qquad (1.19)$$

All these conditions are satisfied if $C_1 = 0$ and $C_2 = -C_3$. Hence, the particular solution satisfying the boundary conditions (1.18) is

$$\alpha = C_2(\xi^{m_2} - \xi^{m_3}) \qquad (1.20)$$

A deflection occurs whatever the value of k_1 or k. Hence, the case $a = 0$ is always unstable. Let us examine the significance of expression (1.20). If $k < 2/(3\sqrt{3}) = 0.3849$, the exponents m_2 and m_3 are real and negative; hence, the slope α is infinite at the leading edge. For $k > 2/(3\sqrt{3})$ the exponents are complex conjugates, and we may write

* The notation Re means "real part of."

$$\alpha = C'\xi^\beta \sin(\gamma \log \xi) \qquad (1.21)$$

with $\beta = -(z_1/2) - 1;\quad \gamma = (1/2)\sqrt{3z_1^2 - 4}$

In this case the slope oscillates between negative and positive values an infinite number of times as we approach the leading edge, while the amplitude tends to infinity or zero, depending on whether $\beta < 0$ or $\beta > 0$.

We may therefore conclude that the infinite instability of the infinitely sharp leading edge is due to the singular behavior of the mathematical solution and the breakdown of the assumptions of linearity on which the theory is based. The actual physical stability must depend on the interplay of two factors. One of these factors is the departure of the aerodynamic forces from the linearized expressions assumed in the present theory. The other factor is the departure from linearity of the geometry of finite deflections and deformations. Further studies, both theoretical and experimental, are necessary to determine the stability where such factors as nonlinearity must be taken into account. It may be concluded that the stability will not only depend on the relative bluntness a, but on the absolute size of the leading edge—i.e., on a scale factor.

(2) Amplification Factor for Lift and Overturning Moment of a Wedge

In the previous paragraph we have considered only the stability problem. For further extension of the theory it is useful to examine what happens when the root of the wedge is given a certain angle of attack, under conditions where the wedge is still stable. Because of the tendency for the leading edge to curl up under a positive angle of attack α_0, the overturning moment N at the root is greater than the value of this moment if the wedge were rigid. In the case of a rigid wedge the moment would be

$$N_0 = (M^2/\sqrt{M^2-1})\rho c^2 l^2 \alpha \qquad (2.1)$$

The ratio of the actual moment N to the rigid wedge moment N_0 is equal to an amplification factor that has been evaluated for various values of the bluntness a. This has been done in more detail in references 2 and 3. By solving the wedge problem as above with a boundary condition that the root is rotated by an angle α_0 and computing the bending moment N at the root, it is found that the amplification factor

$$R_N = N/N_0 \qquad (2.2)$$

may be represented empirically as

$$R_N = [1 - A_1(k/k_c) - B_1(k/k_c)^2]/[1-(k/k_c)] \qquad (2.3)$$

when k is the parameter defined in the previous section and k_c is the critical value of this parameter for instability. This parameter is a function of a through the value of k_c represented by curve A of Fig. 3.

The coefficients A_1 and B_1 are also functions of k_c. We have

$$\left.\begin{aligned} A_1 &= 0.325/k_c \\ B_1 &= 0.250/k_c^2 \end{aligned}\right\} \qquad (2.4)$$

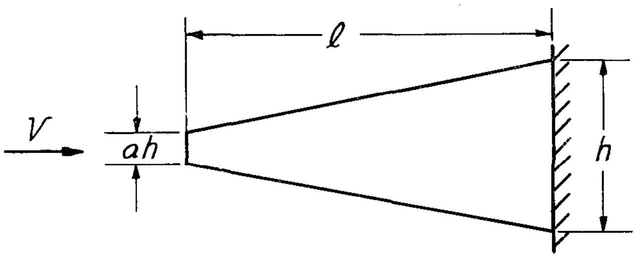

FIG. 1. Straight wedge in the two-dimensional problem.

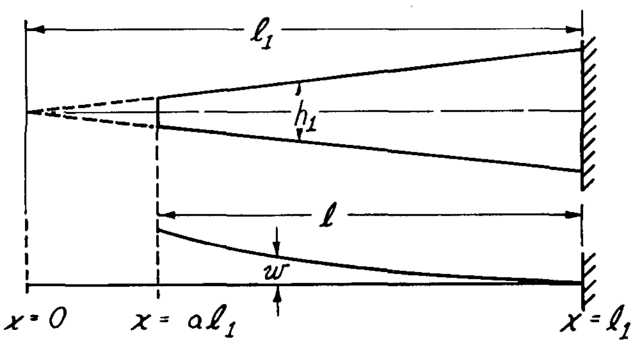

FIG. 2. Coordinates for the wedge.

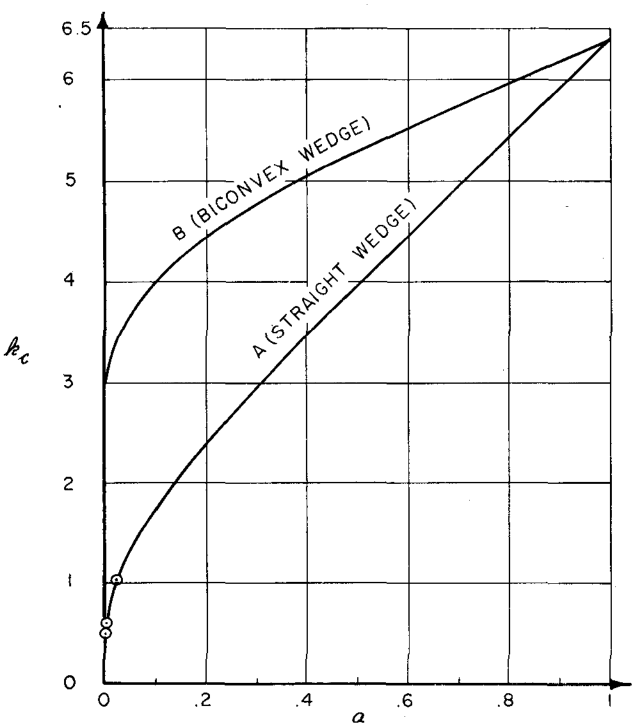

FIG. 3. Critical value of the stability parameter for the straight wedge (A) and biconvex wedge (B).

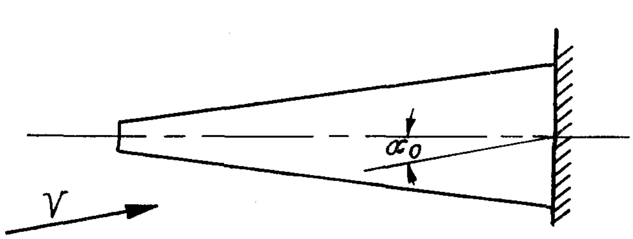

FIG. 4. Wedge with initial angle of attack.

TABLE 1

Critical Value of the Stability Parameter, k, for the Two-Dimensional Straight Wedge as a Function of Bluntness Factor, a

a	k_c
$0 + \epsilon$	.384
.000076	.528
.0204	1.04
.069	1.51
.1055	1.79
.177	2.25
.241	2.63
.460	3.78
.582	4.39
.660	4.74
.712	4.99
.823	5.51
.981	6.27
1.000	6.33

TABLE 2

Critical Value of the Stability Parameter, k, for the Two-Dimensional Biconvex Wedge as a Function of Bluntness Factor, a

a	k_c
0.005	3.06
0.01	3.22
0.02	3.37
0.05	3.69
0.20	4.46
0.50	5.34
1.00	6.33

A similar derivation may be made for the lift L. If the wedge were rigid, the lift would be

$$L_0 = (2M^2/\sqrt{M^2 - 1})\rho c^2 l\alpha \tag{2.5}$$

Defining an amplification factor for the lift as before, we write

$$R_L = L/L_0 \tag{2.6}$$

Again an approximate empirical expression for this factor may be found and written

$$R_L = [1 - A_2(k/k_c) - B_2(k/k_c)^2]/[1 - (k/k_c)] \tag{2.7}$$

with the constants

$$A_2 = 0.15 + (0.40/k_c)$$

$$B_2 = 0.160/k_c$$

The empirical values given above break down, of course, as we approach the case $a = 0$. However, they are reasonably good down to the value of $a = 0.02$.

(3) Stability of the Biconvex Leading Edge

In order to evaluate the influence of the shape of the cross section, let us now investigate the stability of the leading edge of biconvex cross section as shown in Fig. 5.

The problem is treated in reference 4. Unfortunately, it does not lend itself to a closed mathematical solution as the previous case. The boundaries of the profiles are assumed parabolic so that the moment of inertia per unit span is distributed according to the formula

$$I = (h^3/12)\ [1 - (x/l_1)^2]^3 \tag{3.1}$$

The problem is conveniently formulated by means of an integral equation. In order to facilitate the solution from the standpoint of numerical accuracy, it is useful to distinguish between two cases. One case is that of a relatively blunt profile such that for instance $a > 0.2$. The other case is for the sharper leading edge where $a < 0.2$. In the latter case we may expect the singular behavior of the leading edge to become increasingly important as the sharpness increases. In order to take this effect into account, we separate the profile into two parts. One section, A (Fig. 6), which is near the leading edge, is assumed to behave similarly to a straight wedge as considered in Sections (1) and (2) above. The base of the wedge A is taken to be $a'h$ with $a' = 0.2$. The effect of this wedge is then replaced by its moment and lift on the remaining part B of the profile. The integral equation for the slope may be written as follows:

$$\alpha(\xi) = \frac{k}{(\sqrt{1-a})^3}\int_0^{\sqrt{1-a'}} \gamma(\xi,\eta)\alpha(\eta)d\eta + k\alpha_n \frac{l_1}{l}\frac{l''}{l}\left[\frac{R_N}{2}\frac{l''}{l}F_1(\xi) + R_L\frac{l_1}{l}F_2(a',\xi)\right] \tag{3.2}$$

In this expression the eigenvalue parameter k is the same as defined for the straight wedge.

$$k = 24\ (M^2/\sqrt{M^2 - 1})\ (\rho c^2/E_1)\ (l/h)^3 \tag{3.3}$$

The variable ξ is

$$\xi = x/l_1 \tag{3.4}$$

The kernel for $\xi < \eta$ is

$$\gamma(\xi,\eta) = \frac{1}{4}\frac{\xi\eta}{(1-\xi^2)^2} + \frac{3}{8}\frac{\xi\eta}{(1-\xi^2)} + \frac{3}{16}\eta\log\frac{(1+\xi)}{(1-\xi)} - \frac{1}{4}\frac{1}{(1-\xi^2)^2} + \frac{1}{4} \tag{3.5}$$

and for $\xi > \eta$

$$\gamma(\xi,\eta) = \gamma(\eta,\eta)$$

α_n is the slope at the abscissa $x = l'$, ($\xi = \sqrt{1-a'}$).

We also have the functions

$$\left.\begin{aligned} F_1(\xi) &= \int_0^{\xi}\frac{d\xi}{(1-\xi^2)^3} = \frac{1}{4}\frac{\xi}{(1-\xi^2)^2} + \frac{3}{8}\frac{\xi}{1-\xi^2} + \frac{3}{16}\log\frac{1+\xi}{1-\xi} \\ F_2(a',\xi) &= \int_0^{\xi}\frac{\sqrt{1-a'}-\xi}{(1-\xi^2)^3}d\xi = \frac{1}{4}\frac{\xi\sqrt{1-a'}}{(1-\xi^2)^2} + \frac{3}{8}\frac{\xi\sqrt{1-a'}}{1-\xi^2} + \frac{3}{16}\sqrt{1-a'}\log\frac{1+\xi}{1-\xi} - \frac{1}{4}\left(\frac{1}{1-\xi^2}\right)^2 + \frac{1}{4} \end{aligned}\right\} \tag{3.6}$$

The factors R_N and R_L are amplification factors for part A of the profile. They express the fact that if the slope is α_n at $x = l'$, the partial wedge A produces a lift and moment greater than if it were rigid. These factors are given by expressions (2.3) and (2.7). However, we must remember that the parameters in these expressions now refer to the wedge of base $a'h$ and leading edge thickness ah. The bluntness factor of this wedge A is therefore

$$a'' = a/a' \tag{3.7}$$

The stability parameter, k, in Eqs. (2.3) and (2.7) must also be replaced by

$$k'' = k(l''/l)^3\ [1/(a')^3] \tag{3.8}$$

The critical value, k_c, in these formulas is that corresponding to the bluntness a''.

The integral equation (3.2) is a rather complex one since the unknown eigenvalue, k, appears nonlinearly in R_N and R_L. However, it may be conveniently solved by an iteration procedure that is rapidly convergent.

In this iteration process a value k is assumed, say, k_a, from which the amplification factors R_N and R_L are derived. The unknown function, $\alpha(\xi)$, is then represented by an interpolation formula of the type

$$\alpha(\xi) = \alpha_0 \frac{(\xi - \xi_1)(\xi - \xi_2)\ldots(\xi - \xi_n)}{(\xi_0 - \xi_1)(\xi_0 - \xi_2)\ldots(\xi_0 - \xi_n)} + \alpha_1 \frac{(\xi - \xi_0)(\xi - \xi_2)\ldots(\xi - \xi_n)}{(\xi_1 - \xi_0)(\xi_1 - \xi_2)\ldots(\xi_1 - \xi_n)} + \ldots + \alpha_n \frac{(\xi - \xi_0)(\xi - \xi_1)\ldots(\xi - \xi_{n-1})}{(\xi_n - \xi_0)(\xi_n - \xi_1)\ldots(\xi_n - \xi_{n-1})} \quad (3.9)$$

The integral equation is thus replaced by an algebraic system with n unknowns, α_i, and an eigenvalue parameter, k, which may be solved by the usual iteration process. Good accuracy is obtained with $n = 3$ or 4. The new value, k, is then compared with the originally assumed value k_a. If k is not close enough to k_a, the process is repeated a number of times, and, by plotting k versus k_a (Fig. 7), we obtain a curve whose intersection with the straight line $k = k_a$ at P gives the true eigenvalue $k = k_c$. For cases of bluntness, $a \geq 0.2$, the terms containing R_N and R_L drop out of the integral equation. The process is then much simpler and requires only one iteration sequence.

The values k_c for the critical stability parameter, k, as a function of the bluntness a are given in Table 2. The curve of k_c versus a is plotted in Fig. 3, curve B. It is noticed that the biconvex wedge is considerably more stable at the low values of a than the straight wedge.

(4) Approximate Treatment of the Three-Dimensional Problem

The three-dimensional problem of a cantilever wing is obviously a very complex one. Before treating the problem more elaborately, it is useful to bring out certain characteristic features of the phenomena by means of an approximate method. We shall use here a modified "strip method." That is, we shall assume that the wing consists of a series of chordwise strips that are linked together at the mid-chord by a spar. The chordwise bending of these strips and their rotation resulting from the torsional deformation of the spar are the elastic parameters to consider in such a model (Fig. 8). An approach along these lines has been developed in reference 3.

The significant effect to be introduced is the overturning moment due to the curling-up of the strip. This may be done quantitatively by using the results obtained in Section (2) on the overturning moment of a wedge.

Let us assume a double wedge symmetric cross section of chord $2l$ and maximum thickness h. Consider the forward half of the strip (Fig. 9). When the root at the mid-chord rotates through an angle α, the strip bends upward due to the lift distribution. The root moment N on this half strip is according to Eq. (2.2).

$$N = R_N N_0 \quad (4.1)$$

where
$$N_0 = (M^2/\sqrt{M^2 - 1})\,\rho c^2 l^2 \alpha \quad (4.2)$$

and
$$R_N = \frac{1 - A_1(k/k_c) - B_1(k/k_c)^2}{1 - (k/k_c)} \quad (4.3)$$

The root moment due to the aft portion of the strip may similarly be written

$$N' = R_N' N_0 \quad (4.4)$$

with
$$R_N' = \frac{1 + A_1(k/k_c) - B_1(k/k_c)^2}{1 + (k/k_c)} \quad (4.5)$$

The expression for R_N' is taken to be the same as for R_N except for a reversal in sign of the quantity k. This finds its justification in the fact that the deformation of the aft portions of the strip is expressed by a differential equation identical with that [Eq. (1.5)] of the forward portion except for a change in sign of the parameters k and k_1.

In practice the $B_1(k/k_c)^2$ term turns out to be usually small except for very thin leading edges. We shall neglect it hereafter and write:

$$R_N = 1 - A_1(k/k_c)/[1 - (k/k_c)] \quad (4.6)$$

$$R_N' = 1 + A_1(k/k_c)/[1 + (k/k_c)] \quad (4.7)$$

The above expressions have been derived for the aerodynamic forces on a very thin wing. It is possible, however, to introduce the effect of the finite thickness of the wedge by remembering that the so-called "slope of the lift curve" will be different for the forward portion of the wedge and for the aft portion. In other words, we may introduce to this effect correction factors β and β' and write:

$$\left.\begin{aligned} N &= \beta R_N N_0 \\ N' &= \beta' R_N' N_0 \end{aligned}\right\} \quad (4.8)$$

The total unbalanced moment at the mid-chord is

$$N - N' = (\beta R_N - \beta' R_N')\, N_0 \quad (4.9)$$

We will now show that the values of the coefficients β and β' may be derived in terms of the eccentricity of the aerodynamic center. We remember that for a completely rigid structure $k = 0$ and

$$R_N = R_N' = 1$$

Hence, for such a structure

$$N - N' = (\beta - \beta')\, N_0 \quad (4.10)$$

represents the mid-chord moment.

Similarly denoting by L and L' the total lift on the fore and aft portions, we may write for the total lift on the rigid section,

$$L + L' = (\beta + \beta')L_0 \quad (4.11)$$

where L_0 is defined by Eq. (2.5). Because of the symmetry we have to a second-order approximation

$$\beta + \beta' = 2 \quad (4.12)$$

$$L + L' = 2L_0 \quad (4.13)$$

Introducing the eccentricity ϵ of the aerodynamic center as a fraction of the total chord $2l$, we write

$$N - N' = 4\epsilon l L_0 \quad (4.14)$$

also from Eq. (4.10)

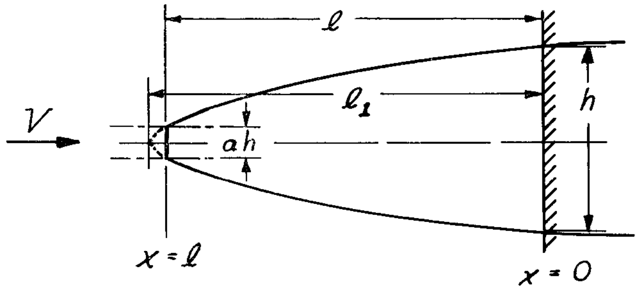

FIG. 5. Biconvex wedge.

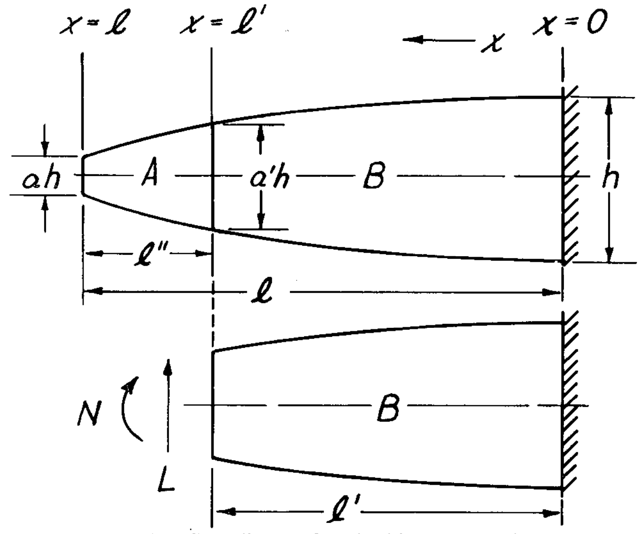

FIG. 6. Coordinates for the biconvex wedge.

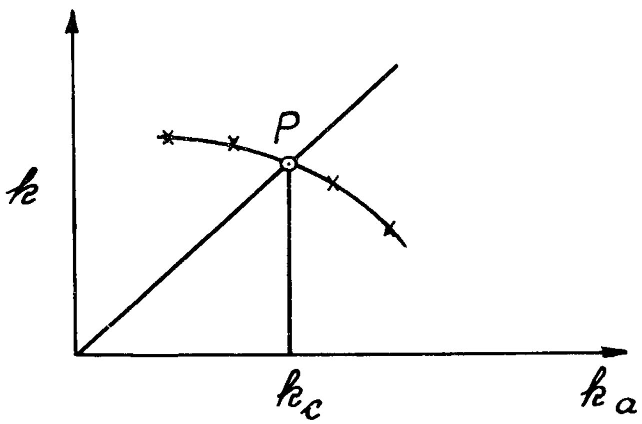

FIG. 7. Plot to determine critical value of k.

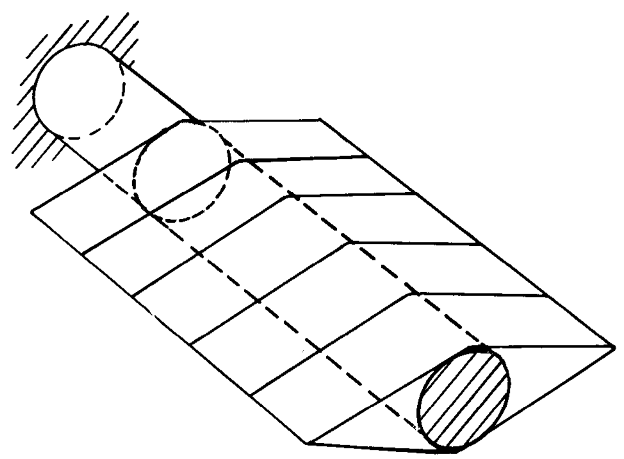

FIG. 8. Wing replaced by a series of chordwise strips.

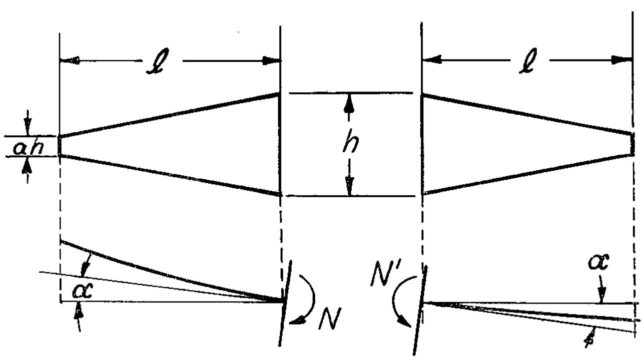

FIG. 9. Moments on fore and aft portions of strip.

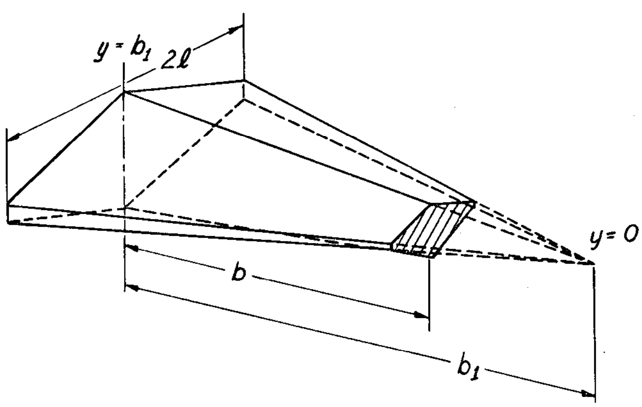

FIG. 11. Cantilever wing of trapezoidal plan form.

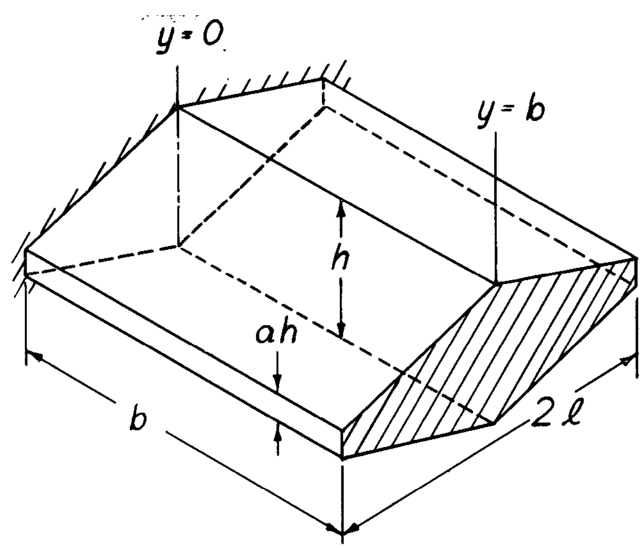

FIG. 10. Cantilever wing of rectangular plan form.

TABLE 3
Critical Value of the Stability Parameter, λ, for the Cantilever Wing of Trapezoidal Plan Form, as a Function of Taper Ratio, $(b_1 - b)/b_1$, as Given by the Strip Theory

$\frac{b_1 - b}{b_1}$	λ
$0 + \epsilon$	1.5
.1	1.66
.2	1.67
.3	1.68
.5	1.65
.7	1.62
1	$\frac{\pi}{2}$

$$(\beta - \beta')N_0 = 4\epsilon l L_0 \tag{4.15}$$

and from Eqs. (2.1) and (2.5)

$$2N_0 = L_0 l \tag{4.16}$$

Hence,
$$(\beta - \beta') = 8\epsilon \tag{4.17}$$

Going back to expression (4.9) and taking into account the values of β and β' derived from Eqs. (4.12) and (4.17), we find for the mid-chord moment of a flexible strip the expression

$$N - N' = \frac{C + A(k/k_c) - B(k/k_c)^2}{1 - (k^2/k_c^2)} N_0 \tag{4.18}$$

with

$$A = 2(1 - A_1)$$
$$B = 8\epsilon A_1$$
$$C = 8\epsilon$$
$$A_1 = 0.325/k_c$$

We now derive a differential equation for the spanwise deformation of the wing. We denote by Q the torsional stiffness of the wing and write:

$$(d/dy)\ [Q(d\alpha/dy)] + N - N' = 0 \tag{4.19}$$

where y is the coordinate along the span. On the other hand

$$N - N' = K\alpha \tag{4.20}$$

with

$$K = \frac{[C + A(k/k_c) - B(k/k_c)^2]\ M^2}{[1 - (k^2/k_c^2)]\sqrt{M^2 - 1}} \rho c^2 l^2 \tag{4.21}$$

Hence, the differential equation for α is

$$(d/dy)\ [Q(d\alpha/dy)] + K\alpha = 0 \tag{4.22}$$

We shall apply this equation to the treatment of two cases.

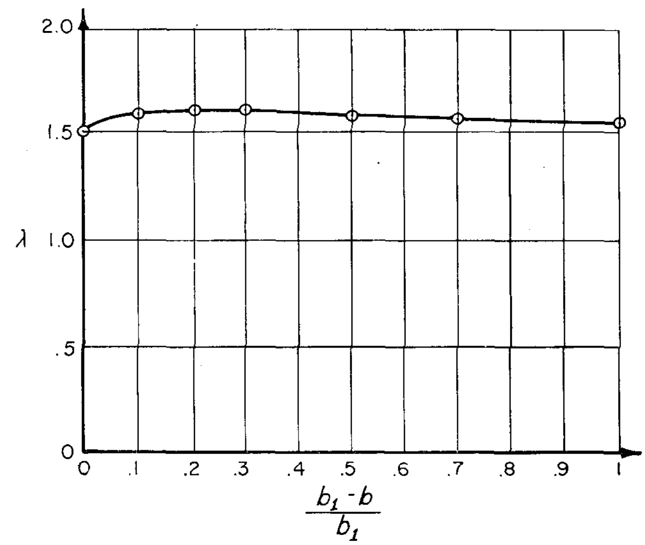

FIG. 12. Stability curve of trapezoidal wing.

The first one considered is that of the cantilever wing of rectangular plan form (Fig. 10). The span is b. We must solve Eq. (4.22) with the boundary conditions

$$\alpha = 0 \quad \text{for} \quad y = 0$$
$$d\alpha/dy = 0 \quad \text{for} \quad y = b$$

A solution satisfying the first boundary condition is

$$\alpha = \sin \sqrt{K/Q}\ y \tag{4.23}$$

The second boundary condition is satisfied if

$$b\sqrt{K/Q} = \pi/2 \tag{4.24}$$

This equation may be written

$$\frac{C + A(k/k_c) - B(k/k_c)^2}{1 - (k/k_c)^2} k(b/l)^2 \frac{E_1 h^3 l}{24Q} = \frac{\pi^2}{4} \tag{4.25}$$

It is an equation for the unknown stability parameter k. Remember that k_c is a known function of a (the bluntness factor of the leading edge), according to the results of Section (1), and given by curve A of Fig. 3. Numerical values are discussed in later sections for comparison with more exact methods. The second example is that of a wing of trapezoidal plan form with no sweep (Fig. 11). All cross sections are assumed similar so that the wing is actually a truncated cone. The origin of the coordinates is taken at the vertex of the cone (at a distance b_1 from the root). The differential equation of the torsional deflection is then

$$(d/dy)\ [Q(y^4/b_1^4)\ (d\alpha/dy)] + K(y^2/b_1^2)\ \alpha = 0 \tag{4.26}$$

where Q is the torsional stiffness at the root and K the value given by Eq. (4.21) in which l is the half root chord.

The general solution of Eq. (4.26) is

$$\alpha = C_1 y^{n_1} + C_2 y^{n_2} \tag{4.27}$$

n_1 and n_2 may be found by substituting in the differential equation. Introducing this solution into the differential equation and applying the boundary conditions, the critical value of the stability parameter

$$\lambda^2 = b^2 \frac{K}{Q} = \frac{C + A(k/k_c) - B(k/k_c)^2}{1 - (k/k_c)^2} k \times \left(\frac{b}{l}\right)^2 \frac{E_1 h^3 l}{24Q} \quad (4.28)$$

is obtained. Critical values of λ are given as a function of the taper ratio, $(b_1 - b)/b_1$, in Table 3 and are plotted in Fig. 12. The taper ratio $(b_1 - b)/b_1 = 1$ corresponds to the rectangular wing analyzed above, and the value of λ for that case is found to be in accordance with Eq. (4.25).

It is interesting to note that the stability is rather insensitive to taper ratio except at very small values of this ratio. The stability is theoretically indeterminate for a conical wing of triangular plan form. This spurious result is analogous to that found in Section (1) for an infinitely sharp leading edge and is due to a breakdown of the physical assumptions.

(5) Application of Linear Plate Theory to the Three-Dimensional Problem

If we restrict ourselves to the simplifying assumption for the aerodynamic forces that the lift is proportional to the local slope, as we have done all along, the stability problem of the plate of uniform thickness may be solved rigorously in some ideal cases which we shall now discuss. The treatment of such cases has the advantage of bringing out certain features that would otherwise have passed unnoticed. Developments are given in more detail in reference 5.

The aeroelastic differential equation for the plate may be written

$$\nabla^4 w + (k/l^3)(\partial w/\partial x) = 0 \quad (5.1)$$

with $\quad [(\partial^2/\partial x^2) + (\partial^2/\partial y^2)]^2 = \nabla^4$

w = plate deflection and l = reference length.

The following problem has been considered. A plate of uniform thickness h, chord $2l$, and span S, is hinged at both ends, $y = 0$ and $y = S$. The mid-chord, $x = 0$, is hinged about a rigid spar. The divergence deformation will then occur as shown in Fig. 13. The fore and aft portions are treated as two different plate problems, connected by the conditions that the deflection is zero at $x = 0$ and that the slope is continuous on that line.

Boundary conditions at the leading and trailing edges are

$$\left.\begin{aligned} (\partial^2 w/\partial x^2) + [\nu(\partial^2 w/\partial y^2)] &= 0 \\ (\partial^3 w/\partial x^3) + (2 - \nu)\,[\partial^3 w/(\partial x \partial y^2)] &= 0 \end{aligned}\right\} \quad (5.2)$$

(ν denotes Poisson's ratio). The first of these conditions corresponds to the vanishing of the bending moment, while the second corresponds to the vanishing of the vertical shear. It is known that the vanishing of the twisting moment is a redundant condition and need not be independently introduced (see reference 1, page 89). The deflection, w, of the plate is expressed in the form

$$\left.\begin{aligned} w_1^{(1)}(\zeta) \sin \lambda y \\ w_1^{(2)}(\zeta) \sin \lambda y \end{aligned}\right\} \quad (5.3)$$

where the first expression refers to the portion ahead of the mid-chord and the second to the portion aft. The chordwise variable is taken as $\zeta = (x/l)\sqrt[3]{k}$. The condition that the wing is pinned at both ends is satisfied if we put $\lambda = \pi/S$, where S denotes the span.

Expressions (5.3) are solutions of the differential equation [Eq. (5.1)] if we write

$$\left.\begin{aligned} w_1^{(1)} &= c_1^{(1)} e^{z_1\zeta} + c_2^{(1)} e^{z_2\zeta} + c_3^{(1)} e^{z_3\zeta} + c_4^{(1)} e^{z_4\zeta} \\ w_1^{(2)} &= c_1^{(2)} e^{z_1\zeta} + c_2^{(2)} e^{z_2\zeta} + c_3^{(2)} e^{z_3\zeta} + c_4^{(2)} e^{z_4\zeta} \end{aligned}\right\} \quad (5.4)$$

The c_i's are eight constants of integration and z_1, z_2, z_3 and z_4 are the four roots of the equation

$$(z^2 - p^2)^2 + z = 0 \quad (5.5)$$

with $\quad p = \pi^2 l^2/(k^{2/3} S^2) \quad (5.6)$

The characteristic determinant for the eigenvalues yields a functional relationship between k and p with an infinite number of branches. The numerical evaluations of these branches have been done for a value of Poisson's ratio, $\nu = 0.3$. From this plot it is possible to find the characteristic values of k for a given aspect ratio, $S/(2l)$. It is found that there are a finite number of real and positive values of k and that this number decreases as the aspect ratio becomes smaller. However, no matter how small the aspect ratio, there always remains one fundamental mode with a real root. Further results presented below indicate that even this real root becomes infinite for a vanishing aspect ratio when Poisson's ratio is zero. For the case $\nu = 0.3$ we have plotted the lowest critical value of k as a function of $S/(2l)$ shown as the full line in Fig. 14.

It is of interest to apply to the present case the strip method as developed in the previous section. Considering that we have a wing hinged at both ends instead of a cantilever, relation (4.24) is replaced by

$$S\sqrt{K/Q} = \pi \quad (5.7)$$

We also introduce the assumption of linear aerodynamic theory—i.e., $\epsilon = 0$ so that $B = C = 0$. Furthermore, for the plate of uniform thickness $a = 1$ and $k_c = 6.33$. Hence, $Ak_c = 12$ and Eq. (5.7) is written

$$\frac{12k^2}{k_c^2 - k^2}\left(\frac{S}{2l}\right)^2 \frac{E_1 h^3 l}{24Q} = \frac{\pi^2}{4} \quad (5.8)$$

The torsional stiffness Q is

$$Q = (1/3)E_1(1 - \nu)h^3 l \quad (5.9)$$

Introducing this value in Eq. (5.8) and solving for k, we find an expression for the critical value as a function of the aspect ratio, for $\nu = 0.3$.

$$k = k_c/\sqrt{1 + 0.87\,(S/2l)^2} \quad (5.10)$$

This value is plotted as a dotted line in Fig. 14. We may conclude from the comparison with the exact value that the strip method yields a good approximation in the present case for high aspect ratio and that the result is still significant down to aspect ratio two. Below aspect ratio one, the strip method completely breaks down.

Another case that has been treated is that of a plate of uniform thickness hinged at both ends, as in the previous case, with a free leading edge but a trailing edge whose deflection is restrained elastically. It is found that as the restraint of the trailing edge is gradually relaxed, the stability increases and becomes very high and very sensitive to the Poisson ratio. In fact, it can be shown that in the case with zero trailing-edge restraint, the instability is completely controlled by the anticlastic effect—i.e., the curling-up of the leading edge caused by the spanwise bending. Since this effect disappears for a zero Poisson ratio, we may expect that, in this case, the plate free at the leading and trailing edges is never unstable. This is effectively the case.

The anticlastic effect may be evaluated independently by considering the plate of infinite chord and span S (Fig. 15). The stability parameter must now be referred to the span and is conveniently taken as p, defined above by Eq. (5.6). We may write

$$\pi^3/p^{3/2} = 24\,(M^2/\sqrt{M^2-1})\,(\rho c^2/E_1)\,(S/h)^3 \tag{5.11}$$

The critical value of p is found to be a function of the Poisson ratio only, according to the curve in Fig. 16.

From this result it may be inferred that in the case of a wing pinned at both ends, an increase in Poisson's ratio will cause an increase of the instability as a result of the anticlastic effect. The critical value of p, as plotted for the infinite chord, is found to check with that found for the limiting case of a wing of the type shown in Fig. 13 whose aspect ratio tends to zero. When both Poisson's ratio and the aspect ratio tend to zero, the wing is found to be infinitely stable. The type of wing illustrated by Fig. 13 contains a spar at the mid-chord which is infinitely flexible in torsion and infinitely rigid in bending. It is interesting to see what happens when this spar is not present and the wing is reduced to a strip of uniform thickness simply hinged at both ends. As already mentioned for the case of a strip of vanishing restraint at the trailing edge, the analysis leads to the striking result that the stability of such a strip depends primarily on Poisson's ratio—i.e., that it is due only to the anticlastic effect. When Poisson's ratio vanishes, the strip becomes infinitely stable. It is obvious that in this case the method of Section (4) completely breaks down since its application would lead to a finite value of the critical parameter in all cases.

As a general conclusion we may therefore state that in addition to the aspect ratio there are two other significant parameters in the stability. One of these parameters is the ratio of the spanwise bending stiffness at the mid-chord to the chordwise bending stiffness (for instance, as measured by the parameter a). The other is the Poisson ratio which controls the anticlastic effect. It will be noted that the latter will have a positive or negative effect on the stability, depending on whether the wing is supported at both ends or cantilevered. In the case of a cantilever, for instance, the anticlastic effect will tend to increase the stability, while for the case of a wing supported at both ends, it will have a tendency to decrease the stability.

(6) The Stability of the Cantilever Wing A General Numerical Method

We shall now consider a case close to the actual practice and solve the problem of the stability of a cantilever wing of symmetric double wedge cross section and rectangular plan form, as shown in Fig. 10 [see Section (4)]. Since we are dealing here with numerical methods, certain specific values of the parameters had to be chosen. The bluntness factor was taken to be

$$a = 0.1$$

This value was assumed to lead to representative results as may be inferred from the analysis of Section (1). Two values of the aspect ratio were also considered

$$\mathcal{R} = b/2l = 1.5,\ 3$$

(b = cantilever span, $2\,l$ = chord).

The Poisson ratio was kept variable. It was first attempted to deal with this problem by using the influence coefficients of the wing as a function of the two coordinates in its plane. The development of this approach is the object of reference 6. However, that method turned out to be less flexible and practical than the one developed hereafter. Only essential points are presented. Further details will be found in reference 7. Essentially what was done was to represent the wing deflections as a sum of amplitudes of "modal functions" and to take the coefficients multiplying these modal functions as generalized coordinates. As an example we show how this method can be applied to the problem of a clamped wedge, treated in Section (1). We may adopt for this deflection w, a polynomial expression

$$w = c_2x^2 + c_3x^3 + \ldots \tag{6.1}$$

The origin of the coordinate x is located at the mid-chord with the leading edge at $x = l$. The coefficients, c_i, are taken as generalized coordinates. The elastic potential energy is

$$V = \frac{1}{2}\int_0^l B(x)\left(\frac{d^2w}{dx^2}\right)^2 dx$$

$$B(x) = (E_1h^3/12)\,[1 - (1-a)\,(x/l)]^3 \tag{6.2}$$

$$E_1 = E/(1-\nu^2)$$

The Lagrangian generalized aerodynamic forces, Q_i, are

$$Q_i = \frac{4M^2}{\sqrt{M^2-1}}\,\frac{\rho c^2}{2}\int_0^l \frac{dw}{dx}\,x^i dx \tag{6.3}$$

Lagrange's equations are thus written:

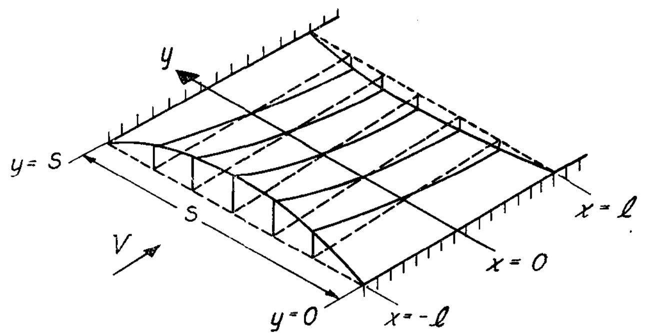

FIG. 13. Wing hinged at both ends and pinned at mid-chord.

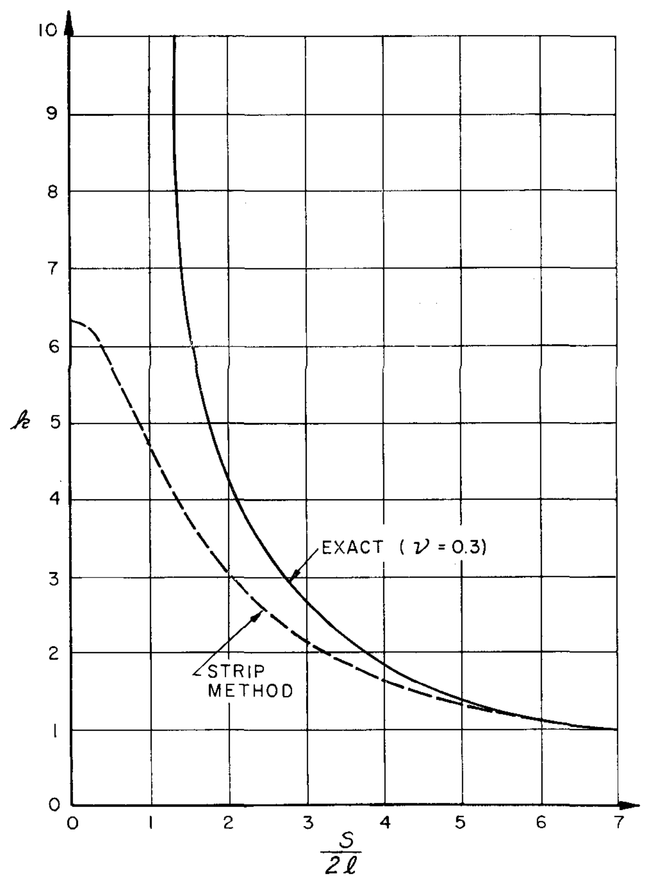

FIG. 14. Stability of the wing illustrated in Fig. 13 as a function of aspect ratio.

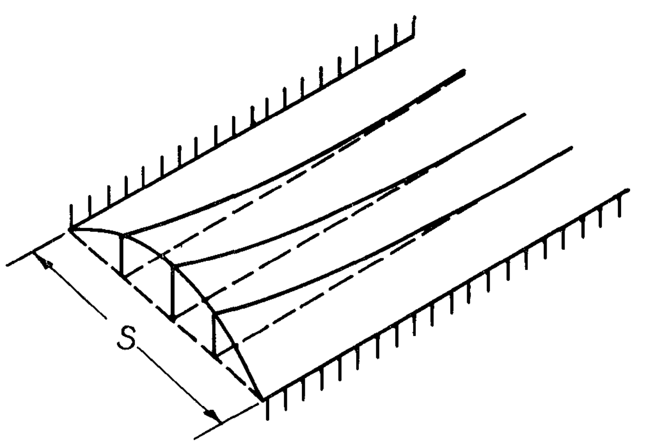

FIG. 15. Wing of infinite chord hinged at both ends.

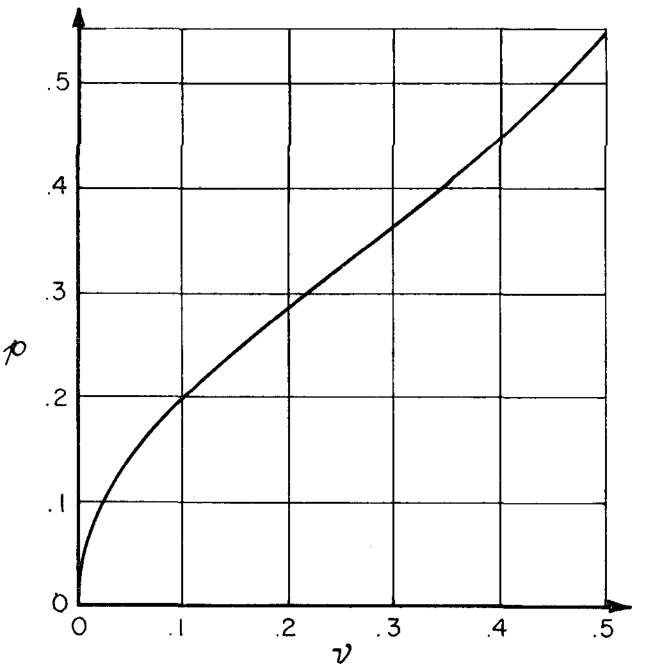

FIG. 16. Stability of the wing of infinite chord illustrated in Fig. 15 as a function of Poisson's ratio.

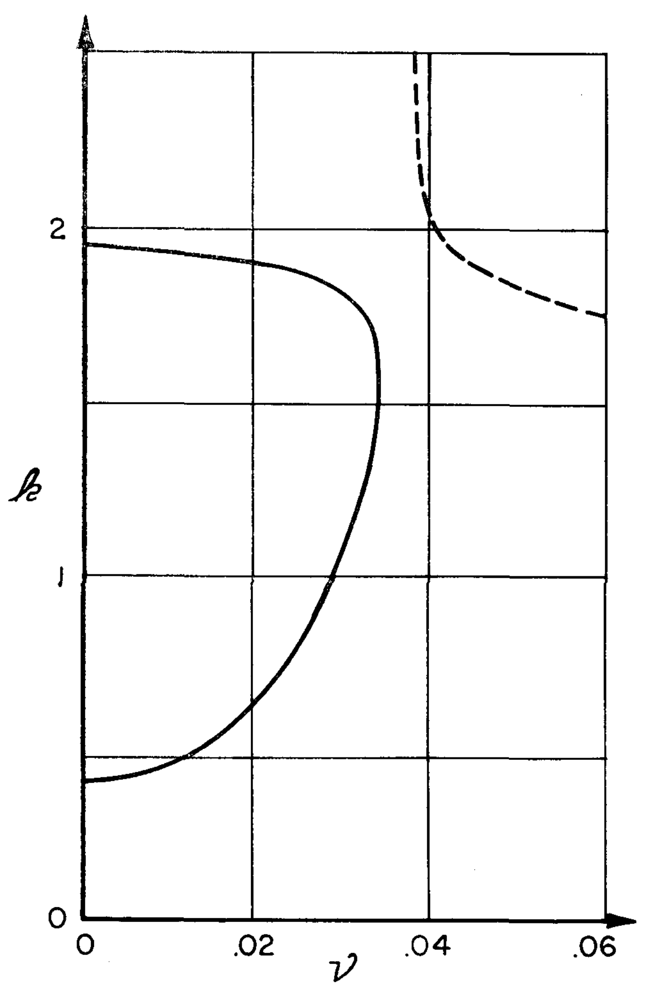

FIG. 17. Stability of a cantilever wing as a function of Poisson's ratio for aspect ratio 3.

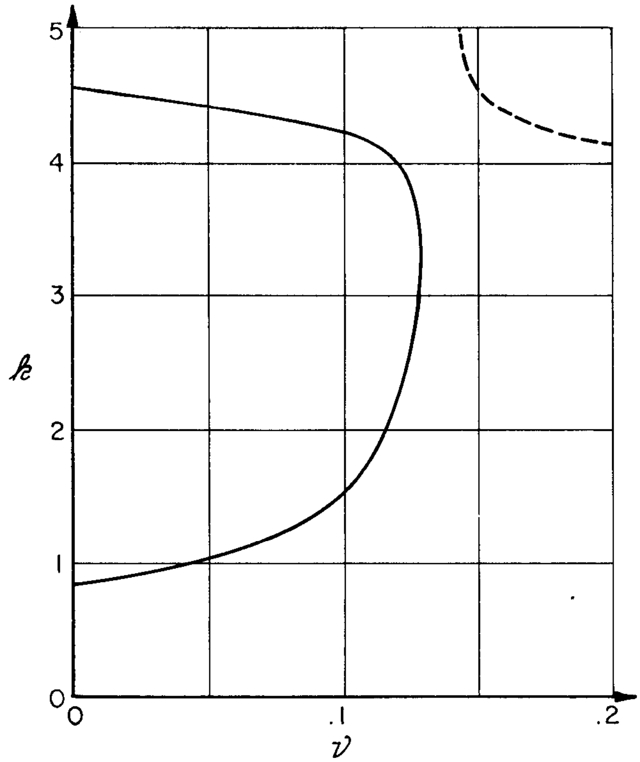

FIG. 18. Stability of a cantilever wing as a function of Poisson's ratio for an aspect ratio 1.5.

$$\partial V/\partial c_i = Q_i \tag{6.4}$$

which in matrix form becomes:

$$\lambda[\psi]\ [c_i] = [\phi]\ [c_i] \tag{6.5}$$

with $\lambda = 1/k$, and where $[\psi]$ and $[\phi]$ are two numerical matrices. The equivalent system

$$\lambda[c_i] = [\psi^{-1}\phi]\ [c_i] \tag{6.6}$$

may conveniently be solved by iteration. For a bluntness of $a = 0.1$, a satisfactory value, $k = 1.78$, is found with only two coefficients, c_2 and c_3, different from zero. For sharper wings, more coordinates have to be used.

The three-dimensional case is then treated in a similar way. The success of this approach and its practicability depends, of course, entirely on the choice of the proper modal functions. In this choice we have been guided by the results obtained above by other methods. A great many types of modal functions have been tried.[7] The following representation of the deflection was used:

$$w = g_1(x)f_1(y) + g_2(x)f_2(y) \tag{6.7}$$

with

$$g_1(x) = c_0 + c_1x + c_2x^2$$

$$f_1(y) = y^2(3b - y)$$

$$g_2(x) = r_1x + r_2x^2$$

$$f_2(y) = y(2b - y)$$

For the coordinate system we refer to Fig. 10. As before, the leading edge is at $x = -l$ and the trailing edge at $x = +l$. The term $g_1(x)f_1(y)$ represents mainly a cantilever deflection with a horizontal slope at the root $y = 0$ and a vanishing curvature at the tip, $y = b$. The term $g_2(x)f_2(y)$ corresponds to a torsional deformation such that $df_2/dy = 0$ at the tip. It will be noted that this deflection does not satisfy the condition of complete clamping at the root along the whole length of the chord but only at the mid-chord. However, it was verified[7] that for the numerical cases investigated here the additional condition of complete clamping does not modify the result appreciably. The procedure then followed is to set up Lagrange's equation using the five coordinates c_0, c_1, c_2, r_1, r_2. The potential energy is expressed by

$$V = \frac{1}{2}\int_{-l}^{l}\int_{0}^{b} B\ [w_{xx}^2 + w_{yy}^2 + 2\nu w_{xx}w_{yy} + 2(1 - \nu)\ w_{xy}^2]\ dx\ dy \tag{6.8}$$

with

$$w_{xx} = \partial^2 w/\partial x^2; \quad w_{xy} = \partial^2 w/(\partial x \partial y), \text{ etc.}$$

and $B = E_1h'^3/12$, where h' is the local wing thickness. The generalized force associated with c_i is

$$Q_{ci} = \frac{4M^2}{\sqrt{M^2 - 1}}\frac{\rho c^2}{2}\int_{-l}^{l}\int_{0}^{b} w_x f_1(y) x^i\ dx\ dy \tag{6.9}$$

and the force associated with r_i is

$$Q_{ri} = \frac{4M^2}{\sqrt{M^2 - 1}}\frac{\rho c^2}{2}\int_{-l}^{l}\int_{0}^{b} w_x f_2(y)\ x^i dx\ dy \tag{6.10}$$

with $\quad w_x = -\partial w/\partial x$

Lagrange's equations are then expressed in a form similar to Eq. (6.5).

$$\lambda[\psi]\ [\Gamma] = [\phi]\ [\Gamma] \tag{6.11}$$

where $[\Gamma]$ is the column matrix of the coordinates, c_i and r_i, and

$$\lambda = 1/k$$

The matrix equation [Eq. (6.11)] was solved for the case $a = 0.1$ and an aspect ratio $b/2l = 3$. The characteristic equation of Eq. (6.11) after elimination of the root $\lambda = 0$ turns out to be a quadratic in λ^2. When the two roots are plotted as a function of the Poisson ratio ν, it is found that we start with two positive real values for $\nu = 0$. This corresponds to two positive values of k. These roots become coincident around $\nu = 0.03$. For higher values of ν the roots first become complex and then become real again, but one root, λ^2, is positive and the other negative. This leads to only one positive value of k. The plot of the stability parameter k versus Poisson's ratio ν is shown for aspect ratio $= 3.0$ in Fig. 17. An identical procedure was used to compute the case of aspect ratio $b/2l = 1.5$, all other parameters being the same. The value of k versus ν for aspect ratio 1.5 is plotted in Fig. 18. The graphs in Figs. 17 and 18 are made of a loop and an asymptotic branch. The latter is indicated by a dotted line, since it is probably spurious and due to the particular choice of generalized coordinates, as may be inferred from the analysis in Section (7).

In discussing these results, let us first consider the case $\nu = 0$. For aspect ratio 3, the lower value of k is found to be $k = 0.406$. Applying the strip method to this case according to the formulas developed in Section (4) and assuming linear aerodynamic forces, we find $k = 0.39$. The two values are close enough to furnish satisfactory evidence that the strip method is applicable to this case. The strip method, however, neglects the anticlastic effect and gives results independent of Poisson's ratio. Inspection of Fig. 17 shows that it completely breaks down beyond a rather small value of Poisson's ratio.

For an aspect ratio of 1.5 in the case $\nu = 0$, the lower value of k is 0.850, while the strip method yields $k = 0.73$. The agreement in this case between the two methods is less satisfactory, as shown by the ordinates for $\nu = 0$ in the plot in Fig. 18. The simplified strip method, as developed in Section (4), does not, of course, yield the dependence of k on Poisson's ratio since it neglects the anticlastic effect. However, in the following section in connection with nonlinearity, the strip method is extended to include the anticlastic effect and the same loop-type curve is derived as in Figs. 17 and 18.

(7) Discussion of Nonlinear Effects

The preceding analysis is restricted to linear theory. This must be understood in the sense that even where the so-called thin wing theory does not apply, either because of wing thickness effects or because of the high Mach Number, the air forces may be linearized in the manner indicated in Section (4). This, however, yields only the incipient instability for very small deflections. It will be shown here that the nonlinear effects become important particularly for thin wings for deflections which in practice may still be considered small, say, of the order of the thickness. There are two important ways in which these nonlinear effects occur; one is through the membrane stresses set up by the anticlastic deformation of the wing, the other is through the aerodynamic forces. We shall first discuss the structural nonlinearity.

Consider again the cantilever wing of rectangular plan form and double wedge cross section of Fig. 10. The y axis is directed along the span b, and the x axis is directed chordwise along the direction of the supersonic flow with the leading edge at $x = -l$ and the trailing edge at $x = l$. If we assume that the major component of the membrane stress is spanwise, σ_y, the membrane stress satisfies the von Karman equation.[15]

$$\partial^2\sigma_y/\partial x^2 = -Eh(w_{xx}w_{yy} - w_{xy}^2) \tag{7.1}$$

This equation applies strictly to constant thickness h but may be used approximately for a variable thickness. We denote by γ the total Gaussian curvature of the middle surface

$$\gamma = w_{xx}w_{yy} - w_{xy}^2 \tag{7.2}$$

If we assume this curvature to be constant along the chord, we may find the chordwise distribution of σ_y. For simplicity we take the wing to be infinitely sharp. The distribution of σ_y is

$$\left.\begin{aligned}
\sigma_y &= \frac{Eh\gamma l^2}{24}\left[-4\left(1+\frac{x}{l}\right)^3 + 12\left(1+\frac{x}{l}\right) - 5\right] \quad \text{for } -l < x < 0 \\
&\text{and} \\
\sigma_y &= \frac{Eh\gamma l^2}{24}\left[-4\left(1-\frac{x}{l}\right)^3 + 12\left(1-\frac{x}{l}\right) - 5\right] \quad \text{for } 0 < x < l
\end{aligned}\right\} \tag{7.3}$$

The constants of integration are determined by the condition that the resultant of all σ_y along the chord is zero. The membrane stress σ_y in conjunction with the spanwise curvature w_{yy} acts as an equivalent load per unit area. The wing deflects as if it were submitted to a total load

$$q' = \sigma_y w_{yy} + q \tag{7.4}$$

where q is the aerodynamic lift given by Eq. (1.1). We shall now compute the chordwise curvature generated by this load. If the curvature w_{xx} is assumed constant along the chord, the deflection due to this curvature is

$$w = (1/2)w_{xx}x^2 \tag{7.5}$$

The value of w_{xx} due to the chordwise load distribution [Eq. (7.4)] may be most conveniently calculated by the method of virtual work. Applying to a strip of unit span expression (6.8) for the elastic energy, we find

$$V = \frac{1}{2}\int_{-l}^{+l} B(w_{xx}^2 + w_{yy}^2 + 2\nu w_{xx}w_{yy})\, dx \tag{7.6}$$

We neglect the twist w_{xy}. Expressing the virtual work due to a variation, δw_{xx}, we have

$$\frac{\partial V}{\partial w_{xx}}\,\delta w_{xx} = \int_{-l}^{+l} q'\,\delta w\, dx \tag{7.7}$$

where $\delta w = (1/2)x^2\delta w_{xx}$. Only the symmetric part of q' contributes to the integral so that we may perform the integration between the limits 0 and l. With an angle of attack, $\alpha = -\partial w/\partial x$, at the mid-chord,

$$w_{xx} + \nu w_{yy} = -(11/15)\,(1 - \nu^2)\,(l^4\gamma/h^2)w_{yy} + (2/3)\,(k\alpha/l) \tag{7.8}$$

Solving for w_{xx}, we may write

$$w_{xx} = -\nu' f w_{yy} + (2/3)\,(fk/l)\alpha \tag{7.9}$$

with

$$\nu' = \nu - (11/15)\,(1 - \nu^2)\,(l^4/h^2)w_{xy}^2 \tag{7.10}$$

and

$$f = 1/[1 + (11/15)\,(1 - \nu^2)\,(l^4/h^2)w_{yy}^2] \tag{7.11}$$

The last two quantities are amplitude dependent. The parameter k is defined by Eq. (1.15).

The chordwise curvature w_{xx} generates an aerodynamic torque per unit length

$$T = \frac{4M^2}{\sqrt{M^2 - 1}} \frac{\rho c^2}{2} \int_{-l}^{+l} x \frac{\partial w}{\partial x} dx \qquad (7.12)$$

with w given by Eq. (7.5). Substituting w_{xx} from Eq. (7.9)

$$T = (4/3)\ [(2/3)fk\alpha - \nu' f l w_{yy}] \times (M^2/\sqrt{M^2 - 1})\ \rho c^2 l^2 \qquad (7.13)$$

The lift per unit span is $2L_0$, where L_0 is defined by Eq. (2.5). Hence, we obtain two spanwise differential equations for torsion and bending

$$\left.\begin{aligned} -(d/dy)\ [Q(d\alpha/dy)] &= T \\ (d^2/dy^2)\ [EI_1(d^2w/dy^2)] &= 2L_0 \end{aligned}\right\} \qquad (7.14)$$

I_1 is the wing cross-section moment of inertia about the chord and Q is its torsional stiffness. If we replace T and L_0 by their values in terms of α and w, these last equations are two simultaneous differential equations for the twist and the deflection as a function of the spanwise coordinate.

Introducing the following dimensionless quantities

$$\left.\begin{aligned} P &= h^3 l E/[24(1 - \nu^2)Q] \\ R &= h^3 l/[6(1 - \nu^2)I_1] \\ \zeta &= w/l \qquad \eta = y/b \\ b &= \text{span} \end{aligned}\right\} \qquad (7.15)$$

for constant values of Q and I_1, the differential equations (7.14) become

$$\left.\begin{aligned} \frac{d^2\alpha}{d\eta^2} + \frac{8}{9} k^2 f P \frac{b^2}{l^2} \alpha - \frac{4}{3} k f \nu' P \frac{d^2\zeta}{d\eta^2} &= 0 \\ (d^4\zeta/d\eta^4) - kR(b^4/l^4)\alpha &= 0 \end{aligned}\right\} \qquad (7.16)$$

The nonlinear character of the phenomenon is contained in the factors f and ν', which become unity and ν, respectively, for small deflections. Strictly speaking, the moment of inertia, I_1, should also be amplitude dependent since the chordwise curvature will stiffen the wing against bending. This will not be introduced explicitly here, but could easily be done. Eliminating ζ, we obtain a single differential equation for the wing twist.

$$(d^4\alpha/d\eta^4) + Hf(d^2\alpha/d\eta^2) - fHS\alpha = 0 \qquad (7.17)$$

with the parameters

$$\left.\begin{aligned} H &= (8/9)k^2P(b^2/l^2) \\ S &= (3/2)\nu' R(b^2/l^2) \end{aligned}\right\} \qquad (7.18)$$

These two parameters embody a similarity law. The boundary conditions for Eqs. (7.16) are

$$\left.\begin{aligned} \alpha &= 0 \quad \text{for } \eta = 0 \\ d\alpha/a\eta = d^2\zeta/d\eta^2 = d^3\zeta/d\eta^3 &= 0 \quad \text{for } \eta = 1 \end{aligned}\right\} \qquad (7.19)$$

Because of the differential equations (7.16), they become

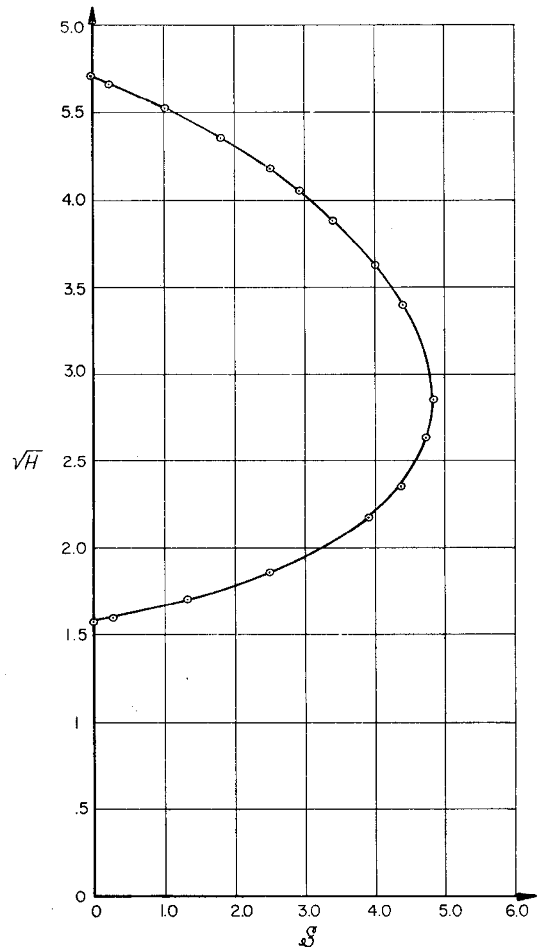

FIG. 19. Dependence of the two basic parameters H and S for stability.

$$\left.\begin{aligned} \alpha &= 0 \quad \text{for } \eta = 0 \\ d\alpha/d\eta &= (d^2\alpha/d\eta^{12}) + \\ fH\alpha &= d^3\alpha/d\eta^3 = 0 \quad \text{for } \eta = 1 \end{aligned}\right\} \qquad (7.20)$$

if we neglect $df/d\eta$ at $\eta = 1$.

It is interesting to examine the linear case for infinitesimal deflection. In this case, $\nu' = \nu$ and $f = 1$, and the differential equation [Eq. (7.17)] has the solution

$$\alpha = C_1 \cos z_1(\eta - 1) + C_2 \cosh z_2(\eta - 1) \qquad (7.21)$$

where z_1 and z_2 satisfy, respectively, the equations

$$z^4 \mp Hz^2 - HS = 0 \qquad (7.22)$$

From the boundary conditions and taking Eq. (7.22) into account, we find

$$\left.\begin{aligned} z_1^2 \cos z_1 + z_2^2 \cosh z_2 &= 0 \\ H &= z_1^2 - z_2^2 \\ S &= z_1^2 z_2^2/(z_1^2 - z_2^2) \end{aligned}\right\} \qquad (7.23)$$

The first equation defines z_2 as a function of z_1, and the last two may be considered parametric equations for H as a function of S. If we plot $\sqrt{H}$ as a function of S, we find a loop as in Figs. 17 and 18. We also find other similar loops in infinite number located above the first, but they are not relevant to the practical range of the parameters. We have plotted the first loop in Fig. 19.

The parameter $\sqrt{H}$ lumps together the value of k with the torsional rigidity and the aspect ratio, $b/2l = Æ$, while S lumps the Poisson ratio ν with the bending rigidity and the aspect ratio. We may derive the loop in Figs. 17 and 18 from the plot of $\sqrt{H}$ versus S and the curves are found to check with an accuracy satisfactory for a first approximation. The bluntness factor a does not appear in this theory but it could be introduced indirectly as in Section (4) by replacing k^2 by $1 - (k^2/k_c^2)$. In this factor k_c is the critical value of k for the two-dimensional wedge problem as developed in Sections (1) and (3).

The effect of finite deformation is obtained by introducing the quantities f and ν', which are amplitude sensitive. If we assume that they are constant along the span, say, equal to some average value, then the effect of finite deformation is obtained by replacing ν by ν' in the expression of S and replacing $\sqrt{H}$ by $\sqrt{Hf}$. A stabilizing influence of finite deformation appears by an increase in the ordinate of $\sqrt{H}$ in the ratio $1/\sqrt{f}$. The replacing of ν by ν' amounts to a decrease of the influence of Poisson's ratio—i.e., a horizontal extension of the unstable area represented by the loop of Fig. 19. Hence, the stabilizing effect of Poisson's ratio, which is effective for infinitesimal deformation, may suddenly disappear at some finite value of the deformation. It can be shown, using expressions for ν' and f, that the effect becomes drastic as soon as the deflection at a spanwise coordinate equal to the chord becomes of the order of the thickness of the wing. It will be safe, therefore, in applying the linear theory to use a zero value of Poisson's ratio.

We must bear in mind here that the influence of finite deformation on the anticlastic bending of thin plates is a bit more complex than assumed in the present approximate theory. As shown by Searle[8] and Ashwell,[9] for a strip of uniform thickness the anticlastic effect becomes confined to a narrow region near the edges. This was also investigated for a double wedge cross section by Fung and Wittrick,[10] Flugge,[11] and Murray and Niles.[12] In this case it is found that the anticlastic effect is confined near the mid-chord.

We shall now consider the possible effect of aerodynamic nonlinearity and, as a consequence, departure from expression (1.1) for the lift. We introduce the expression for the lift, q, given by Hayes[13] and Lighthill[14] for the case of high Mach Number. We may write it

$$q/p_1 = 2\beta\gamma M\alpha \tag{7.24}$$

where

$$\beta = \left(1 + \frac{\gamma + 1}{2} M\delta + \frac{\gamma + 1}{4} M^2\delta^2 + \frac{\gamma + 1}{12} M^2\alpha^2\right) \tag{7.25}$$

with p_1 = pressure of undisturbed gas, δ = slope of symmetric airfoil section relative to the chord, α = angle of attack, and $\gamma = 1.4$ for air. This formula is valid for the range $M(\alpha + \delta) < 1$. The coefficient β is equal to unity for very small values of $M\delta$ and $M\alpha$. In that case, expression (7.24) at high Mach Number coincides with the value [Eq. (1.1)] given by the linear aerodynamic theory. It will be noted that for a double wedge cross section with sharp edge, δ is positive in the fore section and negative for the aft portion while $|\delta|$ is identical with the thickness ratio

$$|\delta| = h/(2l) \tag{7.26}$$

The most significant term in the value of β is $M\delta$, since it will affect the eccentricity of the aerodynamic center and considerably influences the aeroelastic stability. This effect was already taken into account in Section (4) where β was introduced as an empirical factor containing a linear correction term in δ, and β' was the same factor with a negative value of δ.

All analyses made previously may easily be extended by introducing such a factor β with or without the term $M^2\delta^2$, since the aeroelastic theory in that case remains linear. Similar corrections can be introduced in the treatment of Section (6), since the generality of the procedure is not affected. The value of k, for instance, used in Section (1) could be replaced by

$$k = 24\beta\,(M^2/\sqrt{M^2 - 1})\,(\rho c^2/E_1)\,(l/h)^3 \tag{7.27}$$

Finally, the effect of eccentricity of the aerodynamic force can be introduced in the approximate equation [Eq. (7.14)] by writing for T instead of expressions (7.12) the following value

$$T = \left[8\left(\epsilon + \frac{1}{9} fk\right)\alpha - \frac{4}{3}\,\nu' f l w_{yy}\right] \times \frac{M^2}{\sqrt{M^2 - 1}}\,\rho c^2 l^2 \tag{7.28}$$

where ϵ is the eccentricity defined in Section (4).

A truly nonlinear aeroelastic problem appears if we do not neglect the term $M^2\alpha^2$ in the value of β. A rough evaluation of the effect may be obtained by introducing an estimated weighted average of this term for each chordwise strip of the wing and treating β as a constant in each portion. This effect will result in a decrease of stability.

REFERENCES

[1] Timoshenko, S., *Theory of Plates and Shells*, McGraw-Hill Book Co., Inc., 1940.

[2] Biot, M. A., *Aeroelastic Stability of Supersonic Wings, Report No. 1, Chordwise Divergence, The Two-Dimensional Case*, Cornell Aeronautical Laboratory, Inc., Report CAL-CM-427, December 8, 1947.

[3] Biot, M. A., *Aeroelastic Stability of Supersonic Wings, Report No. 2, An Approximate Treatment of Some Simple Three-Dimensional Cases*, Cornell Aeronautical Laboratory, Inc., Report CAL-CM-470, May 12, 1948.

[4] Biot, M. A., *Aeroelastic Stability of Supersonic Wings, Report No. 3, General Method For the Two-Dimension Case and Its Appli-*

cation to the Chordwise Divergence of a Biconvex Section, Cornell Aeronautical Laboratory, Inc., Report CAL-CM-506, September 23, 1948.

[5] Biot, M. A., *Aeroelastic Stability of Supersonic Wings, Report No. 4, Some Exact Solutions Based on Plate Theory*, Cornell Aeronautical Laboratory, Inc., Report CAL-CM-580, November 23, 1949.

[6] Biot, M. A., *Aeroelastic Stability of Supersonic Wings, Report No. 5, Stability of Cantilever Solid Wings of Symmetric Cross-Sections and without Sweep*, Cornell Aeronautical Laboratory, Inc., Report CAL-CM-622, May 31, 1950.

[7] Biot, M. A., *Aeroelastic Stability of Supersonic Wings, Report No. 6, Solution of the Problem by the Use of Generalized Coordinates*, Cornell Aeronautical Laboratory, Inc., Report CAL-CM-730, March 31, 1952.

[8] Searle, G. F. C., *Experimental Elasticity*, Cambridge University Press, 1908.

[9] Ashwell, D. G., *The Anticlastic Curvature of Rectangular Beams and Plates*, Journal Roy. Aero. Soc., Vol. 54, p. 708, 1950.

[10] Fung, Y. C., and Wittrick, W. H., *The Anticlastic Curvature of a Strip with Lateral Thickness Variation*, Journal of Applied Mech., pp. 351–358, December, 1954.

[11] Flugge, W., *Large Deflections of Thin Wings*, Tech. Report No. 3, Air Force Contract No. W 33-038-ac-16697, Stanford University, 1949.

[12] Murray, T. R., and Niles, A. S., *Bending of Wide Beams of Doubly Symmetrical Section*, Tech. Report No. 4, Air Force Con-Contract No. W 33-038-ac-16697, Stanford University, 1949.

[13] Hayes, W., *On Hypersonic Similitude*, Quart. Appl. Math., Vol. 5, pp. 105–106, 1947.

[14] Lighthill, M. J., *Oscillating Airfoil at High Mach Number*, Journal of the Aeronautical Sciences, Vol. 20, No. 6, pp. 402–406, June, 1953.

[15] Love, A. E. H., *The Mathematical Theory of Elasticity*, p. 558; Dover Publications, New York.